Three-dimensional functional workspace of thumb prehension

Article *in* Clinical Biomechanics · February 2019

DOI: 10.1016/j.clinbiomech.2019.02.017

Patrick Curran
University of California, San Francisco

Mitell Sison-Williamson
Shriners Hospitals for Children

Clinical Biomechanics 63 (2019) 63–72

Contents lists available at ScienceDirect

Clinical Biomechanics

journal homepage: www.elsevier.com/locate/clinbiomech

Three-dimensional functional workspace of thumb prehension☆

Patrick F. Curran[a,b], Anita M. Bagley[a], Mitell Sison-Williamson[a], Michelle A. James[a,b,⁎]

[a] Shriners Hospitals for Children Northern California, Sacramento, CA, United States
[b] Department of Orthopaedic Surgery, University of California San Francisco, San Francisco, CA, United States

ARTICLE INFO

Keywords:
Hand biomechanics
Functional thumb motion
Kinematics
Prehension
Motion analysis

ABSTRACT

Background: Clinical assessment of thumb motion is challenging, due to the complex anatomy and motion of the thumb. It is especially difficult to measure hand movement during activity, and to measure the effects of surgery that changes the morphology of the thumb. A three-dimensional model of the hand may enable clinicians to better assess prehension and thumb motion at baseline, and following surgical intervention.
Methods: A kinematic model of the hand was developed to measure thumb and finger position during functional tasks, enabling the calculation of the volume of space in which prehension could occur. This method was validated by application to a mechanical model of the hand, and then applied to ten adult participants, using three-dimensional motion analysis with a marker array developed for the purpose of this study.
Findings: This method can be used to accurately measure three-dimensional thumb joint range of motion (RoM) and predicted functional workspace during functional activities. The thumb carpometacarpal joint was predominantly responsible for thumb position during functional tasks. Predicted functional workspace is proportional to hand morphometric measurements.
Interpretation: A kinematic model of the hand measures thumb RoM and predicts functional workspace during functional activities.

1. Introduction

The thumb plays a critical role in hand function. Patients with impaired thumb structure or mobility, such as in thumb carpometacarpal joint arthritis (Dahaghin et al., 2005; Jones et al., 2001; Zhang et al., 2002), stroke (Arner et al., 2008; Hunter and Crome, 2002), contractures (Bayne, 1985; Flynn, 1956), trauma (Van Oosterom et al., 2005), and congenital hand differences (Manske et al., 1992), have impaired ability to perform activities of daily living (ADLs). Conventional measures of thumb motion have been limited to qualitative assessments and static goniometric measurements (Cooney et al., 1981). A method that measures thumb movement during activities provides objective information that is more likely to reflect the patient's level of disability than routine measures of body structure and function (World Health Organization, 2002), such as static goniometric measurements and pinch strength. In addition, a method that measures the volume of the space in which fingers and thumb can interact, allowing prehension to occur (thumb functional workspace) could measure the effects of surgical treatments that change the morphology of the hand.

Three-dimensional (3D) motion analysis techniques have been used in the upper extremity to measure shoulder, elbow, and wrist function (Fitoussi et al., 2006; Mackey et al., 2006; Mosqueda et al., 2004; Petuskey et al., 2007; Wang et al., 2007). A few studies have applied these techniques to measure hand motion (Buczek et al., 2011; Carpinella et al., 2006; Chang and Pollard, 2008; Goubier et al., 2009; Kuo et al., 2003; Kuo et al., 2009; Metcalf et al., 2008; Tang et al., 2008). However, there is little information in the literature regarding a standard quantitative method to measure 3D thumb joint motion or functional workspace of the hand.

This study presents a 3D model of the hand to measure thumb and finger position. The model presented describes the angular motion of the thumb joint and incorporates a measure of the predicted prehensile reach space (functional workspace of the thumb) (Kuo et al., 2009). The overall goal of the development of this model is to create a method for clinicians to quantify impaired thumb motion and measure treatment efficacy in patients with congenital and acquired thumb conditions. The purpose of this study is to develop, validate, and assess the clinical feasibility of a novel kinematic model of the thumb for measuring thumb joint motion and the functional workspace of prehension.

☆ Funding: This study was funded in part by the POSNA/OREF Research Grant in Pediatric Orthopaedics (Grant number 12-009), United States.
⁎ Corresponding author at: Shriners Hospitals for Children, 2425 Stockton Blvd., Sacramento, CA 95817, United States.
E-mail address: mjames@shrinenet.org (M.A. James).

https://doi.org/10.1016/j.clinbiomech.2019.02.017
Received 20 July 2018; Accepted 26 February 2019

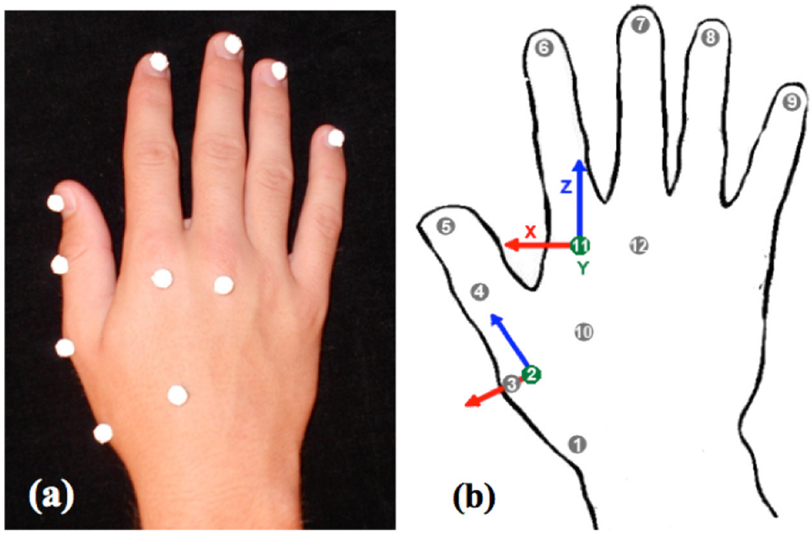

Fig. 1. (a) Markers on control participant. (b) Marker placement and local coordinate system. (1–3) thumb metacarpal; (4) thumb proximal thumb phalanx; (5) thumb distal phalanx; (6–9) finger tip digits 2–5; (10 − 11) 2nd MC; (12) 3rd MC.

2. Methods

2.1. *Joints/segments of interest and degrees of freedom (Kontaxis Clin Biomech 2009)*

The biomechanical model consists of four segments (hand, first metacarpal, first proximal phalanx, and first distal phalanx) whose local coordinate systems are used to calculate hand motion (Fig. 1, Table 1; Kontaxis et al., 2009). Markers on the fingertips of the second, third, fourth and fifth digits are used to track finger position. To describe the thumb joint motion, conventional definitions of planes and terminology about the thumb were adopted (Buterbaugh and Smith, 1994). The thumb interphalangeal (IP) and metacarpophalangeal (MCP) joints were modeled as hinge joints that contribute primarily to flexion-extension motion. The thumb carpometacarpal (CMC) joint was modeled as a saddle joint with two degrees of freedom related to flexion-extension and abduction-adduction.

2.2. *Marker set-up and placement positions*

A twelve-camera motion analysis system (Motion Analysis Corporation, Santa Rosa, CA USA) was used to capture kinematic data at 120 Hz. Twelve retroreflective markers (diameter = 5 mm) were placed on the thumb, fingers and hand (Fig. 2; Appendix A). Each marker was placed to record the 3D position of key anatomical landmarks (Table 2). The markers were placed to measure thumb, finger, and hand motion with the positions as: (1) centered on dorsal surface at base of thumb metacarpal; (2) centered on dorsal surface of thumb metacarpal head; (3) centered on radial surface of thumb metacarpal head; (4) centered on dorsal surface of thumb proximal phalanx head; (5) centered on distal thumb nail over the distal phalanx head; (6) centered on the distal index finger nail; (7) centered on the distal long finger nail; (8) centered on the distal ring finger nail; (9) centered on the distal small finger nail; (10) centered on the dorsal surface of the base of the index finger metacarpal; (11) centered on the dorsal surface of the head of the index finger metacarpal; (12) centered on the dorsal surface of the head of the long finger metacarpal.

2.3. *Segment coordinate systems and angles*

Marker position data were collected during motion analysis testing relative to the laboratory's global coordinate system. In order to describe motion within the standard planes of the hand, locally defined joint coordinate systems of the hand and thumb were generated. These were defined by calculating offsets from markers to estimated joint centers. The method described within this model applies techniques that have been used reliably in upper and lower extremity kinematic models to determine joint centers (Bell et al., 1990; Rab et al., 2002).

For each joint coordinate system, the axes were defined with x-axis pointing radial, z-axis pointing distal, and the y-axis orthogonal to the plane of the hand (Fig. 1B). The offsets to the joint center were calculated as a fraction of the distance between two markers (Table 1; Appendix A). The magnitude of offsets was determined by direct measurements from adult participants and from anthropomorphic data of hand measurements (Alexander et al., 2010; Snyder, 1977). Segmental motion was then defined as the distal segment relative to the proximal segment in the locally established joint coordinate systems (Table 2). Fingertip marker position and the thumb CMC joint motion were measured relative to the local coordinate system generated from the dorsum of the hand (Kuo et al., 2003).

Table 1
Segment definition for biomechanical model.

Moving segment	Reference segment	Designated joint movement
Thumb metacarpal	Hand	Thumb carpometacarpal joint
Thumb proximal phalanx	Thumb metacarpal	Thumb metacarpophalangeal joint
Thumb distal phalanx	Thumb proximal phalanx	Thump interphalangeal joint
Index finger distal phalanx	Hand	
Long finger distal phalanx	Hand	
Ring finger distal phalanx	Hand	
Small finger distal phalanx	Hand	
Hand	Global	

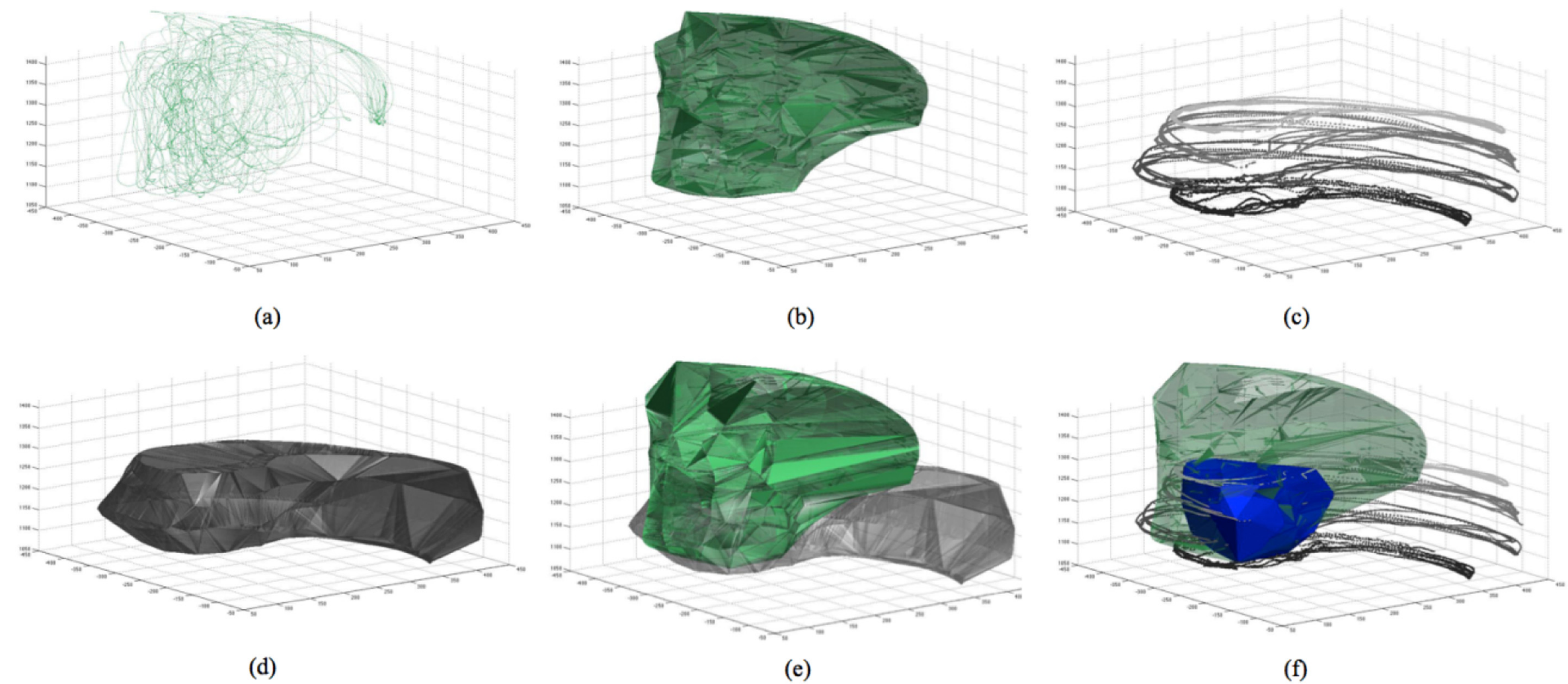

Fig. 2. (a) Thumb range of motion data points. (b) Calculated volume of thumb reach space. (c) Active range of motion of the fingertips. (d) Calculated volume of finger reach space. (e) Thumb and fingertip reach spaces are compared to determine points of intersection. (f) Shared datapoints between the thumb (green) and fingertip (grey) reach spaces are determined and the volume of this space is calculated as previously described (blue). (For interpretation of the references to colour in this figure legend, the reader is referred to the web version of this article.)

Table 2
Offsets to joint centers used for the biomechanical model of the hand (MC = metacarpal; PP = proximal phalanx; DP = distal phalanx; CMC = carpometacarpal; MCP = metacarpophalangeal; IP = interphalangeal).

Joint	Reference marker	Reference segment	Displacement to joint center (%)		
			Radial (x)	Dorsal (y)	Distal (z)
Thumb CMC	Thumb proximal MC	Thumb distal MC	40	−40	0
Thumb MCP	Thumb distal MC	Thumb proximal MC	20	−20	0
Thumb IP	Thumb PP	Thumb distal MC	20	−24	0
Index MCP	Index distal MC	Index proximal MC	0	−18	0

2.4. Activities to be measured: determining functional workspace

Kuo et al. (2009) defined the functional workspace of the thumb as all points in space where the thumb-tip and each fingertip can contact each other. For this study, the thumb functional workspace was calculated by determining the intersection of thumb and fingertip range of motion (RoM); subjects were instructed to move their thumb and fingers through their entire RoM (Fig. 2 and Appendix B). The motion data were then used to generate point cloud of the motion path for the thumb (Fig. 2A) and each fingertip (Fig. 2C). Custom MATLAB software (Natick, Massachusetts, USA) was then used to generate the 3D shell enveloping these data points (Fig. 2B and D). The volume of points within each shell was then interpolated. The shared data points between the thumb and fingertip volumes were calculated and represent the points of potential prehension (Fig. 2F). The resulting volume is defined as the thumb functional workspace.

2.5. Kinematic refinements: joint range of motion and algorithm accuracy

A rigid articulated model of the hand, fingers, and thumb was used to perform an analysis of algorithm accuracy. The model was scaled to the size of an average adult male hand, and constructed from wood and designed to allow movement through hinges placed at the approximate joint centers in the flexion-extension planes of the thumb IP and MCP joints. At the thumb CMC joint, two hinges were affixed to allow flexion-extension and abduction-adduction. The device was placed in the motion system's field of view and a sequence of static thumb positions was recorded. The selected thumb positions incorporated rotation about multiple joints and axes (e.g. CMC abduction followed by CMC flexion and MCP flexion). Data were collected for one-second intervals at 15-degree incremental positions from 0 to 90°. Each trial was performed 3 times. The angle of each joint was averaged over the course of the observed one-second data collection period. The error in RoM measured was calculated as the difference in the expected joint angle as measured by a goniometer and the calculated joint angle by the kinematic model. To study the sensitivity of our method of joint center estimation, the calculated position of the model joint center was perturbed by ± 0.5 cm along each of the three coordinate axes, one axis at a time, and the thumb CMC position was recalculated (Table 3).

2.6. Kinematic refinements: volumetric algorithm accuracy

The volumetric measurements use two algorithms that (1) calculate the volume of thumb or finger reach space and (2) calculate the functional workspace as the intersection of two volumes (thumb and fingertip reach spaces). These algorithms were validated by capturing motion data for known volumes and comparing to calculated volumes. To validate algorithm 1, a marker was moved along a cord of known length through a half sphere of motion (Fig. 3A). For each trial, the marker was moved from 0 to 180° starting at the top of the half sphere and stepping down approximately 10° after each half revolution until reaching the bottom of the half sphere. Each trial was repeated five times. This was then repeated for five total radii of motion: 6.0 cm, 18.5 cm, 38.5 cm, 58.0 cm, 78.0 cm. Custom MATLAB software was used to calculate the hull overlying the captured data points for each trial using Delaunay triangulation (Fig. 3B). The volume within this shape was then calculated for comparison with the predicted value based on the cord length. To validate algorithm 2, the data points from trials with cords of differing lengths were overlaid upon each other (Fig. 3C). The custom MATLAB software was used to determine the points of overlap and output the volume of non-overlapping points (Fig. 3D).

2.7. Range of thumb motion and functional workspace in normal adults

After institutional review board approval, ten participants (five male; average age 28 ± 3.1 years) with no history of upper extremity injury or surgery were recruited as a sample of convenience to serve as control participants. Informed consent was obtained for this study. At enrollment, participant demographics (sex, age, height, weight) and hand morphology (finger segment [phalanx] length, hand length, hand width measured clinically, with a tape measure) were recorded. The study hand was identified as the participant's dominant hand (10 right-hand dominant). Total active ROM of the thumb IP and MCP joints were measured in flexion (F) and extension (E) as well as thumb CMC radial and palmar abduction with a conventional goniometer according to standard technique (Green WB, Heckman JD. The Clinical Measurement of Joint Motion. American Academy of Orthopaedic Surgeons, 1994; Rosemont IL.) Markers were affixed as previously described.

With markers attached, a static neutral positional data was collected to define the initial relative position of each segment of the model. The neutral position was defined with the thumb in the plane of the palm in a position of radial adduction with MCP and IP joints neutral. Each participant then performed a series of trials to measure maximal dynamic ROM of the thumb and motion of the finger-tips: thumb flexion (F), extension (E), opposition (O), radial abduction-adduction (AA), and palmar AA; finger F, E; total thumb ROM; and Kapandji score (Kapandji, 1986), which scores the ability of the subject to touch the pad of the thumb to the pads of each fingertip.

Following ROM trials, 12 activities were performed from a neutral position. Tasks were chosen to represent the types of thumb grasp for common activities of daily living (ADLs): tip pinch (pick up paperclip, pick up penny, pick up paper); tripod pinch (pick up small ball, pick up bottle cap); lateral pinch (grip key); cylinder grip (pick up cup, pick up soup can) and spherical grip (pick up tennis ball) (Table 4). Several of these tasks are components of the Jebsen-Taylor Hand Function Test (Jebsen et al., 1969). Each trial was performed three times and participants were instructed to complete each activity in their own way and at their own pace.

The point of task achievement (PTA) was defined as the terminal point for completion of a task. For example, for the pick-up paperclip task, the PTA was when the participant first grasped the paperclip to pick it up. Joint angle values were recorded for entire tasks and analyzed with the PTA. The positions during activity trials were expressed as mean minimum ROM, mean maximum ROM, and mean PTA for each task (Table 5 and Fig. 4).

The total thumb reach space and functional workspace of the thumb

Table 3
The mean error with (standard deviation) for thumb joint range of motion (in degrees) for validation testing with a rigid articulating model of the hand. Each joint tested joint moved through 15° increments from 0°–90°. The static position of non-tested joints was fixed in either 0° or 45° of position.

CMC F	0–90	0	0	0	45	45	0	0	45	45
CMC Ab	0	0–90	0	45	0	45	0	45	0	45
MCP F	0	0	0–90	0–90	0–90	0–90	0	0	0	45
IP F	0	0	0	0	0	0	0–90	0–90	0–90	0–90
0	0.1 (0.1)	4.6 (4.8)	0.1 (0.1)	0.1 (0.0)	0.1 (0.1)	0.2 (0.1)	2.9 (0.5)	3.8 (0.4)	3.1 (0.6)	5.6 (0.4)
15	1.5 (0.6)	1.1 (0.8)	2.1 (0.6)	1.4 (1.0)	1.4 (1.0)	2.0 (0.8)	0.6 (0.4)	1.9 (0.6)	1.0 (0.6)	2.8 (1.0)
30	2.0 (0.7)	1.4 (0.4)	2.8 (0.5)	1.8 (0.7)	2.4 (0.6)	1.9 (0.3)	0.8 (0.4)	2.8 (0.5)	1.6 (1.0)	2.0 (1.1)
45	2.1 (1.1)	1.2 (0.6)	3.5 (0.8)	1.3 (0.8)	2.7 (1.3)	2.3 (0.6)	0.8 (0.5)	2.2 (0.5)	1.5 (0.7)	1.1 (1.0)
60	1.1 (1.2)	0.9 (0.3)	3.1 (1.0)	1.5 (1.0)	3.2 (0.9)	2.9 (0.6)	1.0 (0.6)	1.7 (0.8)	2.7 (1.2)	1.1 (0.2)
75	1.2 (1.2)	1.3 (1.2)	3.5 (1.3)	1.7 (1.6)	3.5 (0.9)	3.9 (0.9)	2.8 (0.8)	0.8 (0.5)	3.4 (1.3)	0.8 (1.2)
90	1.1 (1.1)	3.3 (1.1)	4.9 (0.8)	3.0 (1.6)	3.5 (0.8)	4.6 (1.1)	3.8 (0.4)	1.9 (1.2)	4.2 (1.4)	1.1 (1.3)
Average	1.3 (0.9)	2.0 (1.3)	2.9 (0.7)	1.5 (1.0)	2.4 (0.8)	2.5 (0.6)	1.8 (0.5)	2.2 (0.6)	2.5 (1.0)	2.1 (0.9)

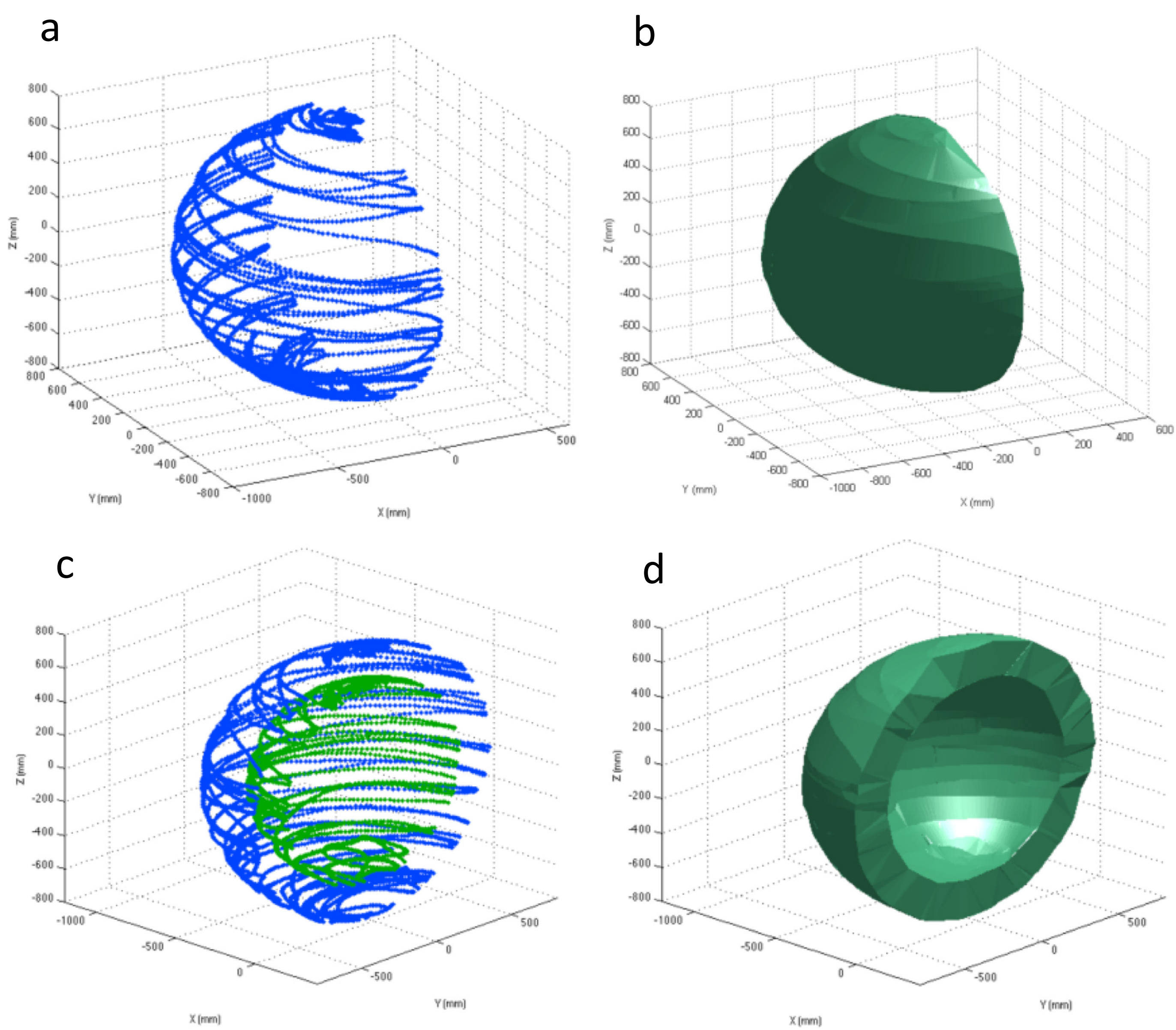

Fig. 3. Validation of reach space algorithms - (a) Data points for outer marker motion through half-sphere. (b) Integrated volume of reach space for outer marker data. (c) Data points for large (blue) and small (green) half spheres. (d) Volume of outer half-sphere with volume of inner half-sphere removed. (For interpretation of the references to colour in this figure legend, the reader is referred to the web version of this article.)

Table 4
Thumb motion with ADLs captured.

Task name	Motion description	Activities captured
Tip	Tip of thumb to tip of index finger	Pick up paperclip, penny, paper
Tripod	Tip of thumb to index and long fingers	Pick up small ball, bottle cap
Lateral pinch	Thumb pad to middle of index finger	Grip key
Cylinder	Pick up cylindrical object with thumb and four fingers	Pick up soup can, cup
Sphere	Pick up spherical object with thumb and four fingers	Pick up tennis ball

was determined for each composite ROM trial as described above.

2.8. Statistical analysis

Descriptive statistics for thumb joint ranges of motion and volumetric measurements were calculated. Percent agreement between goniometric measurements (expected values) and 3D measurements (observed values) is reported as (expected value – observed value) / expected value. One-way analysis of variance (ANOVA) was used for multiple pairwise comparisons in RoM data. Intra-participant variability as defined by the coefficient of variance (CV) was the ratio of the standard deviation to the mean for each volumetric measurement. Significance was set at $p < 0.05$ a priori. Post hoc tests were performed with alpha value for ANOVA = 0.05, using the Bonferroni correction for multiple comparisons (alpha = 0.005) see Table 5 for details.

3. Results

3.1. Joint range of motion and volumetric algorithm accuracy

The mean errors in joint RoM for flexion from a neutral position were 1.3° (SD 0.9°), 2.3° (SD 0.8°), and 2.2° (SD 0.8°) for the CMC, MCP, and IP joints respectively. The mean error in joint RoM for CMC joint abduction was 2.0° (SD 1.3°). The mean errors for joint RoM with other joints not in neutral position were 1.3° (SD 0.9°), 2.9° (SD 0.7°), and 1.8° (SD 0.5°) for the CMC, MCP, and IP joints respectively (Table 3). The mean errors were very small (< 5°) and unlikely to be clinically significant.

The mean percent error between the calculated and predicted volumes of half-sphere motion for algorithm 1 was 3.4% (SD 5.7%). The mean percent error for each cord length was 3.4% (SD 5.7%), 8.3% (SD 8.0%), 1.5% (SD 0.8%), 0.8% (SD 0.5%), and 1.4% (SD 1.3%) for the sphere radius lengths of 6.0 cm, 18.5 cm, 38 cm, 57.5 cm, and 78.0 cm, respectively. There were no significant differences between the calculated and predicted volumes for algorithm 1. The mean percent error between the calculated and predicted volumes for algorithm 2 was 3.5% (SD 3.6%). There were no significant differences between the calculated and predicted volumes for algorithm 2.

3.2. Thumb joint range of motion in normal adults

Thumb ROM data for each type of task are shown in Table 5. Of the 5 types of pinch/grip tested, cylinder grip showed significantly greater ROM in IP and CMC joints. There was no significant difference in MP flexion and extension, and CMC flexion and extension, amongst the pinch/grip types (see Table 5). The points of task achievement data are similarly shown in Table 6. Overall, the CMC joint utilized more of its total ROM (F/E 59.6%, Ab/Ad 50.9%) compared to the IP (F/E 29.6%) and MP (F/E 24.3%) joints. This finding was consistent across all tasks. Figs. 4–7 depict bar graphs for each joint representing the ranges in joint motion required to perform each type of task. These show maximum, minimum, PTA (horizontal line), and one standard deviation for each task.

3.3. Thumb reach space and functional workspace in normal adults

Thumb reach space and functional workspace mean volume data for each participant are shown in Table 7. The coefficient of variance was 7.5% for the thumb reach space and 12.5% for the functional workspace.

4. Discussion

This study presents a method to quantify the three-dimensional ROM of the thumb joints and potential volume of prehension. A kinematic model of the hand was developed to measure thumb and finger position during functional tasks, enabling the calculation of the volume of space in which prehension could occur. This method was validated by application to a mechanical model of the hand, and applied to ten adult participants, using three-dimensional motion analysis with a marker array developed for this purpose. We found that this method can accurately measure three-dimensional thumb joint RoM and predicted prehensile volume, or functional workspace.

Clinical assessment of thumb motion is challenging given the complex anatomy and motion of the thumb, and the fact that many surgical interventions, such as first webspace deepening, ligament reconstruction and tendon interposition for thumb CMC arthritis and thumb MP

Table 5
Thumb joint maximum and minimum ROM during five types of ADLs. Joint motion reported as mean value with standard deviation in parentheses. (IP = thumb interphalangeal joint; MP = thumb metacarpophalangeal joint; CMC = thumb carpometacarpal joint). Post hoc tests (see Section 2.8) showed that for IP flexion and extension, cylindrical grip range of motion was greater than tip pinch range of motion (p = 0.002) or tripod pinch (p = 0.001). For CMC pronation and supination, cylindrical grip range of motion was greater than lateral pinch range of motion (p = 0.005). For CMC abduction and adduction, cylindrical grip range of motion was greater than tip pinch range of motion (p = 0.001), tripod pinch range of motion (p = 0.003), and spherical grip range of motion (p-0.001).

Joint motion (°)	Total ROM	Tip pinch	Tripod pinch	Lateral pinch	Cylinder grip	Spherical grip
IP flexion	70 (19)	2 (12)	10 (12)	13 (19)	15 (10)	13 (21)
IP extension	−32 (12)	−22 (6)	−22 (6)	−18 (9)	−19 (7)	−17 (9)
MP flexion	65 (9)	25 (4)	25 (4)	23 (6)	22 (3)	22 (5)
MP extension	−15 (11)	7 (6)	4 (5)	6 (5)	2 (6)	1 (6)
CMC flexion	46 (5)	41 (4)	40 (4)	33 (7)	42 (5)	38 (7)
CMC extension	−14 (5)	6 (6)	4 (5)	7 (8)	4 (6)	5 (6)
CMC abduction	25 (5)	12 (4)	12 (4)	11 (5)	25 (7)	16 (6)
CMC adduction	−8 (4)	−1 (4)	−2 (4)	−3 (4)	0 (5)	−2 (4)
CMC supination	6 (10)	−2 (4)	0 (8)	−1 (9)	−1 (8)	0 (8)
CMC pronation	−48 (8)	−32 (8)	−33 (9)	−26 (11)	−42 (9)	−32 (11)

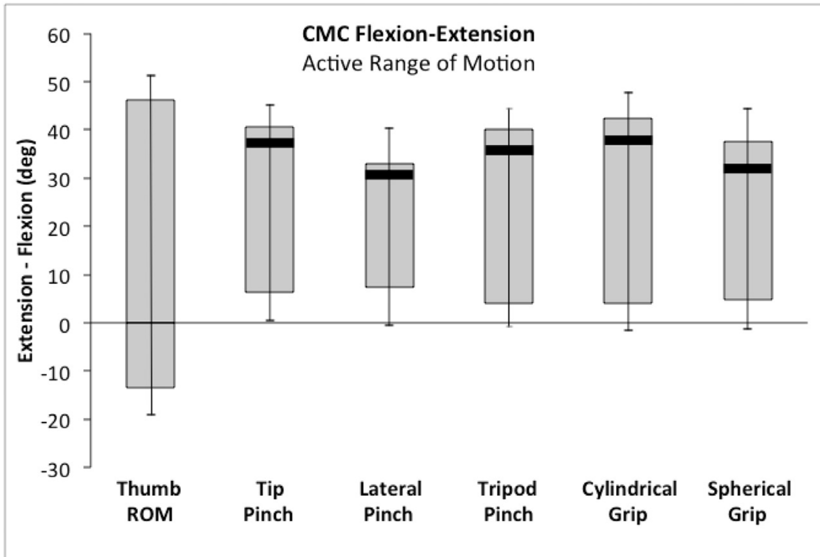

Fig. 4. Bar graph of thumb carpometacarpal (CMC) joint flexion-extension active range during five types of tasks. Includes maximum and minimum values and ± one standard deviation error bar. The mean PTA is designated by a horizontal line.

Table 6
PTA during five types of thumb motion. By convention, positive ROM values are for joint flexion (F), abduction (Ab), and supination (S) whereas negative ROM values are for joint extension (E), adduction (Ad), and pronation (P). Joint motion reported as mean value with standard deviation in parentheses.

Joint motion (°)	Tip pinch	Tripod pinch	Lateral pinch	Cylinder grip	Spherical grip
IP F/E	−14 (6)	−12 (7)	2 (21)	11 (10)	−2 (16)
MP F/E	17 (7)	14 (6)	26 (8)	11 (8)	8 (11)
CMC F/E	37 (4)	36 (5)	31 (9)	38 (7)	32 (9)
CMC Ab/Ad	9 (4)	9 (5)	8 (6)	21 (7)	13 (8)

joint arthrodesis, change the morphology of the thumb. Some thumb reconstructive operations, such as toe to thumb transfer and index pollicization, changes the shape of the hand so drastically that it is difficult to compare standard objective measures before and after treatment. The technique we have described and validated here provides accurate measurement of thumb motion, which may aid in clinical decision making, and quantifies the volume of prehension, which provides a new potentially useful measurement of thumb function that can be compared across conditions and after operations that change morphology. This technique could be applied using standard motion analysis equipment and software.

A few studies have examined in vivo kinematics using 2 dimensional radiographic techniques (Miura et al., 2004). More recently, computer tomography has emerged as an accurate method to measure kinematics of the thumb (Crisco et al., 2015; Goto et al., 2014; Halilaj et al., 2014; Su et al., 2014). While these provide valuable insight into thumb motion, they are limited in their routine clinical application due to radiation exposure. They also usually provide sequential static measurements during simulated activities rather than dynamic motion measurements in real-time, which is a strength of 3D kinematic measurement of thumb functional workspace, as described and validated by our study.

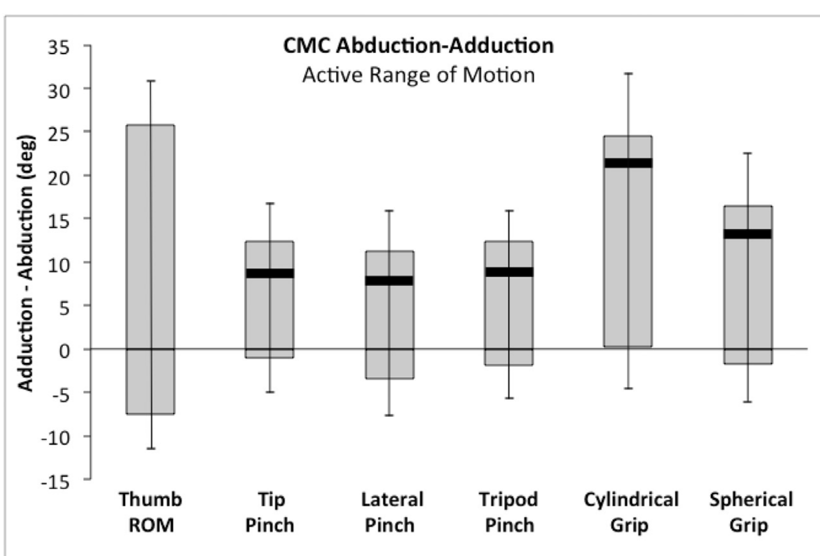

Fig. 5. Bar graph of thumb carpometacarpal (CMC) joint abduction-adduction active range during five types of tasks. Includes maximum and minimum values and ± one standard deviation error bar. The mean PTA is designated by a horizontal line.

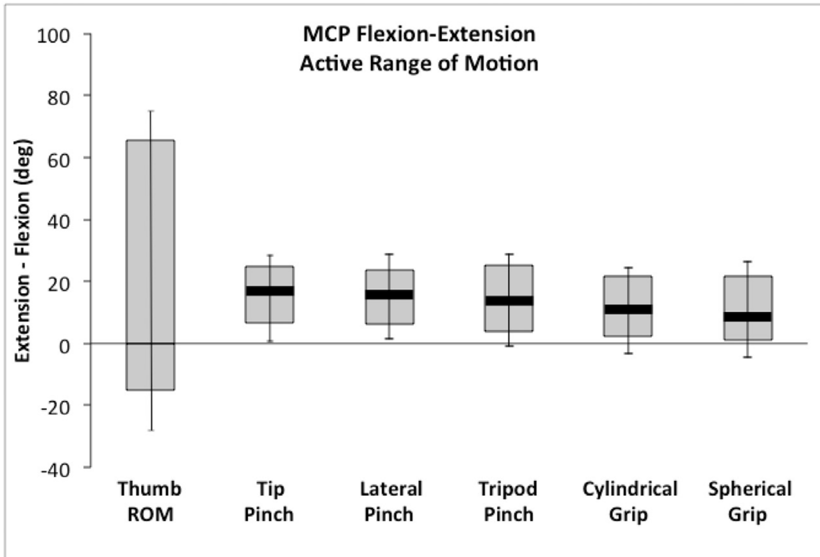

Fig. 6. Bar graph of thumb metacarpophalangeal (MCP) joint flexion-extension active range during five types of tasks. Includes maximum and minimum values and ± one standard deviation error bar. The mean PTA is designated by a horizontal line.

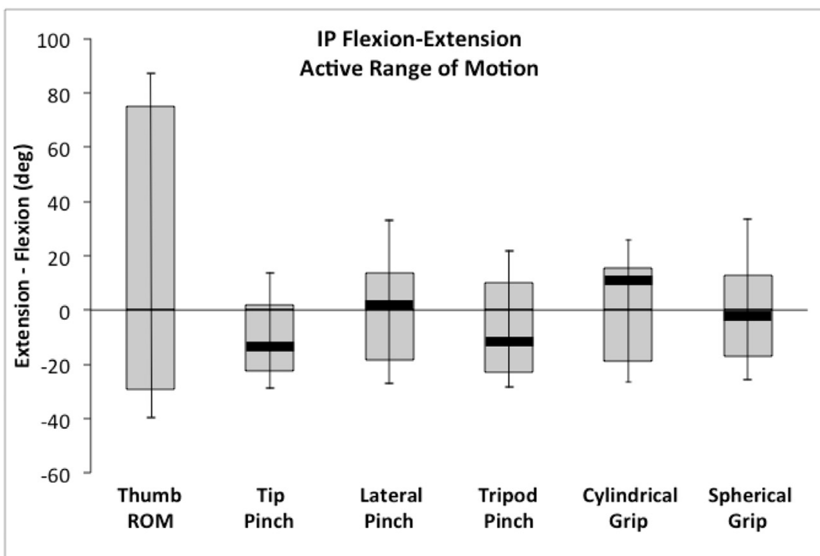

Fig. 7. Bar graph of thumb interphalangeal (IP) joint flexion-extension active range during five types of tasks. Includes maximum and minimum values and ± one standard deviation error bar. The mean PTA is designated by a horizontal line.

Three-dimensional motion analysis techniques used for conventional analysis of the lower extremity have been adapted for the upper extremity, including several models for measurement of hand motion. However, these have not been applied outside of small studies (Buczek et al., 2011; Carpinella et al., 2006; Chang and Pollard, 2008; Goubier et al., 2009; Kuo et al., 2003; Kuo et al., 2009; Metcalf et al., 2008; Tang et al., 2008). The model presented in this study has builds upon these prior studies, combining several key features. First, motion of the thumb CMC joint is measured as initially described by Cooney (Cooney et al., 1981), and thumb and finger motion are referenced to a hand-based coordinate system, rather than affixing the hand to a reference frame (Kuo et al., 2004; Li and Tang, 2007; Tang et al., 2008). This allows capture of activity-based hand motion. Measurement of hand position and motion during activities addresses the activity domain of function according to the World Health Organization International Classification of Functioning, Disability and Health (WHO-ICF) (World Health Organization, 2002) Measurements of body structure (RoM, etc.) provide important baseline information about impairment caused

Table 7
The mean (standard deviation) thumb reach space and functional workspace for each subject.

	S1	S2	S3	S4	S5	S6	S7	S8	S9	S10
Thumb reach space (cm^3)	233 (31)	131 (11)	218 (16)	254 (33)	226 (21)	161 (14)	180 (5)	164 (9)	269 (26)	176 (9)
Functional workspace (cm^3)	66 (5)	35 (4)	50 (8)	73 (18)	44 (6)	34 (5)	32 (1)	43 (6)	52 (7)	44 (11)
Thumb length (cm)	201	178	196	213	195	167	165	165	202	183

by a health condition, but measurements of activity help us understand the impact of this impairment on the patient's ability to perform daily tasks. There are few reproducible methods of measuring motion during activities.

Second, the model decreases marker error and interference by minimizing the number of markers (Buczek et al., 2011; Carpinella et al., 2006; Metcalf et al., 2008), decreasing marker size (Goubier et al., 2009), eliminating marker clusters (Goubier et al., 2009; Kuo et al., 2004; Lin et al., 2011; Tang et al., 2008), and placing markers on key anatomic landmarks.

Third, the model also describes the motion of the thumb joints about clinically relevant planes of motion, similar to those previously reported in the literature (Barakat et al., 2013; Cooney et al., 1981; Goubier et al., 2009; Halilaj et al., 2014; Li and Tang, 2007; Lin et al., 2011; Surgeons, 1965). We found that during completion of functional tasks, the CMC joint contributes predominantly to thumb position, similar to previous motion analysis (Lin et al., 2011) and radiographic studies (Halilaj et al., 2014; Luker et al., 2014).

Measurement of the potential volume of finger and thumb contact may be useful for clinical assessment of patients with hand conditions. Previously, Kuo (Kuo et al., 2004; Kuo et al., 2009) defined the functional workspace of the hand as the area of points in space that the thumb-tip and each fingertip can contact each other. The model presented in this study expands Kuo's concept, by interpolating the volume of space of intersection of the thumb and fingers, rather than predicting a conically shaped thumb volume from a single circumduction task. Similar to the results of this study, Kuo et al. found a relationship between the measured workspace of the thumb and finger or thumb length. For the purpose of this study, hand length is used as a correlate for predicted functional workspace. This enables this model to assess deficiencies in thumb motion in pathologic states, such as seen in children with congenital thumb hypoplasia.

4.1. Study limitations

This study has several limitations. First, we studied normal thumbs of young adult participants, which may limit applicability of our results to other populations. Second, joint motion is determined indirectly, using surface markers. This method is subject to theoretical errors due to soft tissue artifact between the skin, soft tissue, and bone. The degree of measurement error in this model due to soft tissue artifact is unknown, but is likely small due to the thin soft tissue of the hand. Third, this model also describes movement of the thumb metacarpal relative to the hand as a proxy to measure thumb CMC motion. This is due to the relative difficulty of applying surface markers to the trapezium. This model also describes motion of the thumb carpometacarpal joint within orthogonal planes. While these are useful for modeling and intuitive understanding of motion, they may not capture motion along the true anatomic planes of motion of the thumb CMC joint (Crisco et al., 2015; Hollister et al., 1992). Lastly, the offset measurements for joint centers used in this study are based upon estimated joint centers from morphometric surface measurements.

5. Conclusion

This study presents the development, validation, and application of a noninvasive biomechanical model for measuring thumb kinematics and the functional volume of hand prehension. Future studies will apply this model to measure thumb motion in patients with congenital and acquired hand conditions.

CRediT authorship contribution statement

Patrick F. Curran: Conceptualization, Formal analysis, Investigation, Methodology, Validation, Writing - original draft. **Anita M. Bagley:** Conceptualization, Formal analysis, Methodology, Validation, Writing - review & editing. **Mitell Sison-Williamson:** Data curation, Project administration, Supervision. **Michelle A. James:** Conceptualization, Funding acquisition, Methodology, Resources, Supervision, Writing - review & editing.

Acknowledgements

This study was funded in part by the POSNA/OREF Research Grant in Pediatric Orthopaedics (Grant number 12-009), United States.

Appendix A. Supplementary data

Supplementary data to this article can be found online at https://doi.org/10.1016/j.clinbiomech.2019.02.017.

References

Alexander, B., Viktor, K., Buryanov, A., Kotiuk, V., 2010. Proportions of hand segments. Int. J. Morphol. 28 (3), 755–758.
American Academy of Surgeons, 1965. Joint Motion: Method of Measuring and Recording. AAOS, Chicago.
Arner, M., Eliasson, A.C., Nicklasson, S., Sommerstein, K., Hagglund, G., 2008. Hand function in cerebral palsy. Report of 367 children in a population-based longitudinal health care program. J Hand Surg Am 33 (8), 1337–1347.
Barakat, M.J., Field, J., Taylor, J., 2013. The range of movement of the thumb. Hand (N Y) 8 (2), 179–182.
Bayne, L.G., 1985. Hand assessment and management of arthrogryposis multiplex congenita. Clin. Orthop. Relat. Res.(194), 68-73.
Bell, A.L., Pedersen, D.R., Brand, R.A., 1990. A comparison of the accuracy of several hip center location prediction methods. J. Biomech. 23 (6), 617–621.
Buczek, F.L., Sinsel, E.W., Gloekler, D.S., Wimer, B.M., Warren, C.M., Wu, J.Z., 2011. Kinematic performance of a six degree-of-freedom hand model (6DHand) for use in occupational biomechanics. J. Biomech. 44 (9), 1805–1809.
Buterbaugh, G.A., Smith, R., 1994. Function and kinesiology of the thumb. The Thumb. W. P. Strickland. Churchill Livingstone, Edinburgh, pp. 31–43.
Carpinella, I., Mazzoleni, P., Rabuffetti, M., Thorsen, R., Ferrarin, M., 2006. Experimental protocol for the kinematic analysis of the hand: definition and repeatability. Gait Posture 23 (4), 445–454.
Chang, L.Y., Pollard, N.S., 2008. Method for determining kinematic parameters of the in vivo thumb carpometacarpal joint. IEEE Trans. Biomed. Eng. 55 (7), 1897–1906.
Cooney 3rd, W.P., Lucca, M.J., Chao, E.Y., Linscheid, R.L., 1981. The kinesiology of the thumb trapeziometacarpal joint. J. Bone Joint Surg. Am. 63 (9), 1371–1381.
Crisco, J.J., Halilaj, E., Moore, D.C., Patel, T., Weiss, A.P., Ladd, A.L., 2015. Vivo kinematics of the trapeziometacarpal joint during thumb extension-flexion and abduction-adduction. J Hand Surg Am 40 (2), 289–296.
Dahaghin, S., Bierma-Zeinstra, S.M., Ginai, A.Z., Pols, H.A., Hazes, J.M., Koes, B.W., 2005. Prevalence and pattern of radiographic hand osteoarthritis and association with pain and disability (the Rotterdam study). Ann. Rheum. Dis. 64 (5), 682–687.
Fitoussi, F., Diop, A., Maurel, N., Laassel el, M., Pennecot, G.F., 2006. Kinematic analysis of the upper limb: a useful tool in children with cerebral palsy. J Pediatr Orthop B 15 (4), 247–256.
Flynn, J.E., 1956. Adduction contracture of the thumb. N. Engl. J. Med. 254 (15), 677–686.
Goto, A., Leng, S., Sugamoto, K., Cooney 3rd, W.P., Kakar, S., Zhao, K., 2014. In vivo pilot study evaluating the thumb carpometacarpal joint during circumduction. Clin. Orthop. Relat. Res. 472 (4), 1106–1113.
Goubier, J.N., Devun, L., Mitton, D., Lavaste, F., Papadogeorgou, E., 2009. Normal range-of-motion of trapeziometacarpal joint. Chir Main 28 (5), 297–300.
Halilaj, E., Rainbow, M.J., Got, C., Schwartz, J.B., Moore, D.C., Weiss, A.P., Ladd, A.L., Crisco, J.J., 2014. In vivo kinematics of the thumb carpometacarpal joint during three isometric functional tasks. Clin. Orthop. Relat. Res. 472 (4), 1114–1122.
Hollister, A., Buford, W.L., Myers, L.M., Giurintano, D.J., Novick, A., 1992. The axes of rotation of the thumb carpometacarpal joint. J. Orthop. Res. 10 (3), 454–460.
Hunter, S.M., Crome, P., 2002. Hand function and stroke. Rev. Clin. Gerontol. 12 (1), 68–81.
Jebsen, R.H., Taylor, N., Trieschmann, R.B., Trotter, M.J., Howard, L.A., 1969. An objective and standardized test of hand function. Arch. Phys. Med. Rehabil. 50 (6), 311–319.
Jones, G., Cooley, H.M., Bellamy, N., 2001. A cross-sectional study of the association between Heberden's nodes, radiographic osteoarthritis of the hands, grip strength, disability and pain. Osteoarthr. Cartil. 9 (7), 606–611.
Kapandji, A., 1986. Clinical test of apposition and counter-apposition of the thumb. Ann. Chir. Main 5 (1), 67–73.
Kontaxis, A., Cutti, A.G., Johnson, G.R., Veeger, H.E.J., 2009. A framework for the

definition of standardized protocols for measuring upper-extremity kinematics. Clin. Biomech. 24, 246–253.
Kuo, L.C., Cooney III, W.P., Oyama, M., Kaufman, K.R., Su, F.C., An, K.N., 2003. Feasibility of using surface markers for assessing motion of the thumb trapeziometacarpal joint. Clin. Biomech. 18, 558–563.
Kuo, L.C., Cooney 3rd, W.P., Kaufman, K.R., Chen, Q.S., Su, F.C., An, K.N., 2004. A quantitative method to measure maximal workspace of the trapeziometacarpal joint–normal model development. J. Orthop. Res. 22 (3), 600–606.
Kuo, L.C., Chiu, H.Y., Chang, C.W., Hsu, H.Y., Sun, Y.N., 2009. Functional workspace for precision manipulation between thumb and fingers in normal hands. J. Electromyogr. Kinesiol. 19 (5), 829–839.
Li, Z.M., Tang, J., 2007. Coordination of thumb joints during opposition. J. Biomech. 40 (3), 502–510.
Lin, H.T., Kuo, L.C., Liu, H.Y., Wu, W.L., Su, F.C., 2011. The three-dimensional analysis of three thumb joints coordination in activities of daily living. Clin. Biomech. 26 (4), 371–376.
Luker, K.R., Aguinaldo, A., Kenney, D., Cahill-Rowley, K., Ladd, A.L., 2014. Functional task kinematics of the thumb carpometacarpal joint. Clin. Orthop. Relat. Res. 472 (4), 1123–1129.
Mackey, A.H., Walt, S.E., Stott, N.S., 2006. Deficits in upper-limb task performance in children with hemiplegic cerebral palsy as defined by 3-dimensional kinematics. Arch. Phys. Med. Rehabil. 87 (2), 207–215.
Manske, P.R., Rotman, M.B., Dailey, L.A., 1992. Long-term functional results after pollicization for the congenitally deficient thumb. J Hand Surg Am 17 (6), 1064–1072.
Metcalf, C.D., Notley, S.V., Chappell, P.H., Burridge, J.H., Yule, V.T., 2008. Validation and application of a computational model for wrist and hand movements using surface markers. IEEE Trans. Biomed. Eng. 55 (3), 1199–1210.
Miura, T., Ohe, T., Masuko, T., 2004. Comparative in vivo kinematic analysis of normal and osteoarthritic trapeziometacarpal joints. J Hand Surg Am 29 (2), 252–257.
Mosqueda, T., James, M.A., Petuskey, K., Bagley, A., Abdala, E., Rab, G., 2004. Kinematic assessment of the upper extremity in brachial plexus birth palsy. J. Pediatr. Orthop. 24 (6), 695–699.
Petuskey, K., Bagley, A., Abdala, E., James, M.A., Rab, G., 2007. Upper extremity kinematics during functional activities: three-dimensional studies in a normal pediatric population. Gait Posture 25 (4), 573–579.
Rab, G., Petuskey, K., Bagley, A., 2002. A method for determination of upper extremity kinematics. Gait Posture 15 (2), 113–119.
Snyder, R.G., 1977. Anthropometry of Infants, Children, and Youths to Age 18 for Product Safety Design. Final Report.
Su, F.C., Lin, C.J., Wang, C.K., Chen, G.P., Sun, Y.N., Chuang, A.K., Kuo, L.C., 2014. In vivo analysis of trapeziometacarpal joint arthrokinematics during multi-directional thumb motions. Clin. Biomech. 29 (9), 1009–1015.
Tang, J., Zhang, X., Li, Z.M., 2008. Operational and maximal workspace of the thumb. Ergonomics 51 (7), 1109–1118.
Van Oosterom, F.J., Ettema, A.M., Mulder, P.G., Hovius, S.E., 2005. Functional outcome after surgical treatment of phalangeal fractures in severely injured hands. Scand. J. Plast. Reconstr. Surg. Hand Surg. 39 (4), 238–241.
Wang, J.S., Petuskey, K., Bagley, A.M., James, M.A., Rab, G., 2007. The contralateral unimpaired arm as a control for upper extremity kinematic analysis in children with brachial plexus birth palsy. J. Pediatr. Orthop. 27 (6), 709–711.
World Health Organization (2002). Towards a Common Language for Functioning, Disability and Health: ICF. http://www.who.int/classifications/icf/icfbeginnersguide.pdf?ua=1 (accessed April 22, 2018).
Zhang, Y., Niu, J., Kelly-Hayes, M., Chaisson, C.E., Aliabadi, P., Felson, D.T., 2002. Prevalence of symptomatic hand osteoarthritis and its impact on functional status among the elderly: the Framingham Study. Am. J. Epidemiol. 156 (11), 1021–1027.